J|A|C|S
ARTICLES
Published on Web 03/01/2002

Electron-Nuclear Double Resonance Spectroscopic Evidence That *S*-Adenosylmethionine Binds in Contact with the Catalytically Active [4Fe−4S]$^{+}$ Cluster of Pyruvate Formate-Lyase Activating Enzyme

Charles J. Walsby,[†] Wei Hong,[‡] William E. Broderick,[‡] Jennifer Cheek,[‡] Danilo Ortillo,[‡] Joan B. Broderick,*[,‡] and Brian M. Hoffman*[,†]

Contribution from the Department of Chemistry, Northwestern University, Evanston, Illinois 60208-3113, and Department of Chemistry, Michigan State University, East Lansing, Michigan 48824-1322

Received August 23, 2001

Abstract: Pyruvate formate-lyase activating enzyme (PFL-AE) is a representative member of an emerging family of enzymes that utilize iron−sulfur clusters and *S*-adenosylmethionine (AdoMet) to initiate radical catalysis. Although these enzymes have diverse functions, evidence is emerging that they operate by a common mechanism in which a [4Fe−4S]$^{+}$ interacts with AdoMet to generate a 5′-deoxyadenosyl radical intermediate. To date, however, it has been unclear whether the iron−sulfur cluster is a simple electron-transfer center or whether it participates directly in the radical generation chemistry. Here we utilize electron paramagnetic resonance (EPR) and pulsed 35 GHz electron-nuclear double resonance (ENDOR) spectroscopy to address this question. EPR spectroscopy reveals a dramatic effect of AdoMet on the EPR spectrum of the [4Fe−4S]$^{+}$ of PFL-AE, changing it from rhombic (g = 2.02, 1.94, 1.88) to nearly axial (g = 2.01, 1.88, 1.87). ^{2}H and ^{13}C ENDOR spectroscopy was performed on [4Fe−4S]$^{+}$-PFL-AE ($S = {}^{1}/_{2}$) in the presence of AdoMet labeled at the methyl position with either ^{2}H or ^{13}C (denoted [1+/AdoMet]). The observation of a substantial ^{2}H coupling of ∼1 MHz (∼6−7 MHz for ^{1}H), as well as hyperfine-split signals from the ^{13}C, manifestly require that AdoMet lie close to the cluster. ^{2}H and ^{13}C ENDOR data were also obtained for the interaction of AdoMet with the diamagnetic [4Fe−4S]$^{2+}$ state of PFL-AE, which is visualized through cryoreduction of the frozen [4Fe−4S]$^{2+}$/AdoMet complex to form the reduced state (denoted [2+/AdoMet]$_{red}$) trapped in the structure of the oxidized state. ^{2}H and ^{13}C ENDOR spectra for [2+/AdoMet]$_{red}$ are essentially identical to those obtained for the [1+/AdoMet] samples, showing that the cofactor binds in the same geometry to both the 1+ and 2+ states of PFL-AE. Analysis of 2D field-frequency ^{13}C ENDOR data reveals an isotropic hyperfine contribution, which requires that AdoMet lie in contact with the cluster, weakly interacting with it through an incipient bond/antibond. From the anisotropic hyperfine contributions for the ^{2}H and ^{13}C ENDOR, we have estimated the distance from the closest methyl proton of AdoMet to the closest iron of the cluster to be ∼3.0−3.8 Å, while the distance from the methyl carbon to the nearest iron is ∼4−5 Å. We have used this information to construct a model for the interaction of AdoMet with the [4Fe−4S]$^{2+/+}$ cluster of PFL-AE and have proposed a mechanism for radical generation that is consistent with these results.

Introduction

Iron−sulfur clusters in biological systems participate in a broad range of functions, including electron transfer, redox and nonredox catalysis, structural roles, and regulation of gene expression.[1,2] A new role for Fe−S clusters has emerged in recent years as a number of enzymes have been identified that utilize Fe−S clusters and *S*-adenosylmethionine (AdoMet) to generate catalytically essential radicals.[3,4] This class of enzymes has been identified as the "radical *S*-adenosylmethionine" superfamily, with over 600 unique sequences found to date,[5] spanning a diverse range of functions, including generation of stable protein radicals (activating enzymes for pyruvate formate-lyase[6,7] and anaerobic ribonucleotide reductase[8]), cofactor biosynthesis (biotin[9−11] and lipoic acid[12,13] synthases), rearrangement

[†] Northwestern University.
[‡] Michigan State University.

(1) Beinert, H.; Holm, R. H.; Münck, E. *Science* **1997**, *277*, 653−659.
(2) Beinert, H. *J. Biol. Inorg. Chem.* **2000**, *5*, 2−15.
(3) Cheek, J.; Broderick, J. B. *J. Biol. Inorg. Chem.* **2001**, *6*, 209−226.
(4) Frey, P. A. *Annu. Rev. Biochem.* **2001**, *70*, 121−148.
(5) Sofia, H. J.; Chen, G.; Hetzler, B. G.; Reyes-Spindola, J. F.; Miller, N. E. *Nucl. Acids Res.* **2001**, *29*, 1097−1106.
(6) Broderick, J. B.; Duderstadt, R. E.; Fernandez, D. C.; Wojtuszewski, K.; Henshaw, T. F.; Johnson, M. K. *J. Am. Chem. Soc.* **1997**, *119*, 7396−7397.
(7) Külzer, R.; Pils, T.; Kappl, R.; Hüttermann, J.; Knappe, J. *J. Biol. Chem.* **1998**, *273*, 4897−4903.
(8) Ollagnier, S.; Mulliez, E.; Schmidt, P. P.; Eliasson, R.; Gaillard, J.; Deronzier, C.; Bergman, T.; Gräslund, A.; Reichard, P.; Fontecave, M. *J. Biol. Chem.* **1997**, *272*, 24216−24223.
(9) Sanyal, I.; Cohen, G.; Flint, D. H. *Biochemistry* **1994**, *33*, 3625−3631.
(10) Guianvarc'h, D.; Florentin, D.; Bui, B. T. S.; Nunzi, F.; Marquet, A. *Biochem. Biophys. Res. Commun.* **1997**, *236*, 402−406.

Scheme 1. Reaction Catalyzed by Pyruvate Formate-Lyase Activating Enzyme

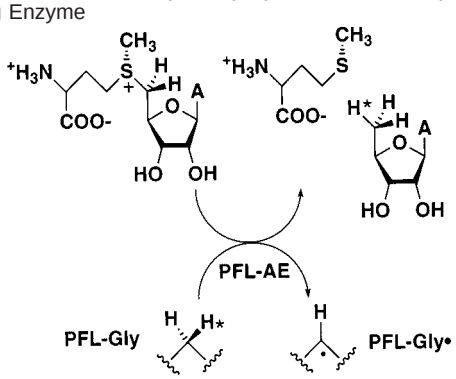

reactions (lysine aminomutase),[14] and DNA repair (spore photoproduct lyase[15]).[3] Pyruvate formate-lyase activating enzyme (PFL-AE), a representative member of this family of enzymes, generates a stable glycyl radical at G734 on pyruvate formate-lyase (PFL) via reductive cleavage of AdoMet, converting AdoMet stoichiometrically to methionine and 5′-deoxyadenosine (5′-dAdo) (Scheme 1).[6,16−18] PFL utilizes the catalytically essential glycyl radical to convert pyruvate and coenzyme A (CoA) to formate and acetyl-CoA, the first committed step in anaerobic glucose metabolism in bacteria such as *Escherichia coli*.[16,17] Isotope labeling experiments established that the pro-S hydrogen atom abstracted from G734 in PFL is incorporated into the methyl group of the 5′-dAdo product, suggesting the presence of a 5′-dAdo radical intermediate during the activation of PFL.[19] The involvement of a 5′-dAdo radical intermediate, produced by the reductive cleavage of AdoMet, appears to be a key mechanistic feature shared by the "radical *S*-adenosylmethionine" superfamily members.[3,4] Elegant work by Frey and co-workers has provided direct spectroscopic evidence for an allylic analogue of the 5′-dAdo radical in lysine aminomutase.[20,21]

A central mechanistic question in PFL-AE, and the radical *S*-adenosylmethionine superfamily in general, is the role the iron−sulfur cluster plays in the reductive cleavage of AdoMet to generate the putative 5′-dAdo radical intermediate. Anaerobically purified PFL-AE contains primarily cuboidal $[3Fe-4S]^{+}$ clusters, with smaller quantities of $[4Fe-4S]^{2+}$, $[2Fe-2S]^{2+}$, and linear $[3Fe-4S]^{+}$ clusters.[18,22] However, this mixture of clusters is converted to $[4Fe-4S]^{2+/+}$ clusters under reducing conditions.[22] Such reductive cluster conversions have been observed for other members of this enzyme family,[11,23] as well as for other iron−sulfur cluster enzymes such as aconitase,[24−27] and are thought to proceed via release of Fe(II) and sulfide from the protein followed by reassembly of the [4Fe−4S] cluster.[28] We previously demonstrated for PFL-AE that the reduced $[4Fe-4S]^{1+}$ form of the iron−sulfur cluster is the catalytically essential and active form, serving as the source of the electron required to reductively cleave AdoMet and generate the G734 glycyl radical on PFL.[29] The details of this unprecedented reaction remain unanswered, including the key question of how the $[4Fe-4S]^{1+}$ cluster interacts with AdoMet, with there being several possibilities. The $[4Fe-4S]^{1+}$ may play a simple electron-transfer role in the reductive cleavage of AdoMet, transferring an electron to AdoMet, which then fragments to methionine and the 5′-dAdo radical. Alternatively, the [4Fe−4S] cluster may be more directly involved in the radical generation reaction, via covalent interactions with AdoMet. This may involve intermediates in which a bridging S or an Fe atom of the cluster interacts with either the sulfonium S or the 5′-adenosyl C of AdoMet, but in any case, AdoMet must bind in close proximity to the [4Fe−4S] cluster. Indirect evidence for such a close interaction of AdoMet with the [4Fe−4S] cluster of lysine aminomutase was reported by Cosper et al.[30] They demonstrated an interaction of ∼2.7 Å between selenomethinione, the turnover product of Se-AdoMet, and an Fe of the [4Fe−4S] cluster by using Se X-ray absorption spectroscopy. No interaction was observed, however, between Se-AdoMet and the iron−sulfur cluster.

To probe the interaction of AdoMet with the [4Fe−4S] cluster of PFL-AE, we have carried out electron paramagnetic resonance (EPR) and 35 GHz pulsed electron-nuclear double resonance (ENDOR)[31] studies of the PFL-AE-AdoMet complex with AdoMet labeled with ^{2}H and ^{13}C at the sulfonium methyl group. ENDOR observations of hyperfine interactions between the ^{2}H and ^{13}C nuclei on AdoMet and the paramagnetic $S = {}^{1}/_{2}$ $[4Fe-4S]^{1+}$ cluster state of PFL-AE, would provide unequivocal direct spectroscopic evidence for a close association of AdoMet with the [4Fe−4S] cluster and information about binding geometry.[32,33] In previous work we demonstrated the ability to reduce PFL-AE to the $[4Fe-4S]^{1+}$ state in good yield via 5′-deazariboflavin-mediated photoreduction.[29] In the present work, we have exploited this approach to prepare samples for ENDOR

(11) Duin, E. C.; Lafferty, M. E.; Crouse, B. R.; Allen, R. M.; Sanyal, I.; Flint, D. H.; Johnson, M. K. *Biochemistry* **1997**, *36*, 11811−11820.
(12) Busby, R. W.; Schelvis, J. P. M.; Yu, D. S.; Babcock, G. T.; Marletta, M. A. *J. Am. Chem. Soc.* **1999**, *121*, 4706−4707.
(13) Miller, J. R.; Busby, R. W.; Jordan, S. W.; Cheek, J.; Henshaw, T. F.; Ashley, G. W.; Broderick, J. B.; Cronan, J. E., Jr.; Marletta, M. A. *Biochemistry* **2000**, *39*, 15166−15178.
(14) Lieder, K.; Booker, S.; Ruzicka, F. J.; Beinert, H.; Reed, G. H.; Frey, P. A. *Biochemistry* **1998**, *37*, 2578−2585.
(15) Rebeil, R.; Sun, Y.; Chooback, L.; Pedraza-Reyes, M.; Kinsland, C.; Begley, T. P.; Nicholson, W. L. *J. Bacteriol.* **1998**, *180*, 4879−4885.
(16) Knappe, J.; Elbert, S.; Frey, M.; Wagner, A. F. V. *Biochem. Soc. Trans.* **1993**, *21*, 731−734.
(17) Wong, K. K.; Kozarich, J. W. *S-Adenosylmethionine-Dependent Radical Formation in Anaerobic Systems*; Sigel and Sigel, Ed.; Marcel Dekker: New York, 1994; Vol. 30, pp 361−404.
(18) Broderick, J. B.; Henshaw, T. F.; Cheek, J.; Wojtuszewski, K.; Trojan, M. R.; McGhan, R.; Smith, S. R.; Kopf, A.; Kibbey, M.; Broderick, W. E. *Biochem. Biophys. Res. Commun* **2000**, *269*, 451−456.
(19) Frey, M.; Rothe, M.; Wagner, A. F. V.; Knappe, J. *J. Biol. Chem.* **1994**, *269*, 12432−12437.
(20) Magnusson, O. T.; Reed, G. H.; Frey, P. A. *J. Am. Chem. Soc.* **1999**, *121*, 9764−9765.
(21) Magnusson, O. T.; Reed, G. H.; Frey, P. A. *Biochemistry* **2001**, *40*, 7773−7782.
(22) Krebs, C.; Henshaw, T. F.; Cheek, J.; Huynh, B.-H.; Broderick, J. B. *J. Am. Chem. Soc.* **2000**, *122*, 12497−12506.
(23) Ollagnier, S.; Meier, C.; Mulliez, E.; Gaillard, J.; Schuenemann, V.; Trautwein, A.; Mattioli, T.; Lutz, M.; Fontecave, M. *J. Am. Chem. Soc.* **1999**, *121*, 6344−6350.
(24) Kent, T. A.; Dreyer, J. L.; Kennedy, M. C.; Huynh, B. H.; Emptage, M. H.; Beinert, H.; Münck, E. *Proc. Natl. Acad. Sci. U.S.A.* **1982**, *79*, 1096−1100.
(25) Emptage, M. H.; Kent, T. A.; Kennedy, M. C.; Beinert, H.; Munck, E. *Proc. Natl. Acad. Sci. U.S.A.* **1983**, *80*, 4674−4678.
(26) Werst, M. M.; Kennedy, M. C.; Beinert, H.; Hoffman, B. M. *Biochemistry* **1990**, *29*, 10526−10532.
(27) Werst, M. M.; Kennedy, M. C.; Houseman, A. L.; Beinert, H.; Hoffman, B. M. *Biochemistry* **1990**, *29*, 10533−40.
(28) Ugulava, N. B.; Gibney, B. R.; Jarrett, J. T. *Biochemistry* **2000**, *39*, 5206−5214.
(29) Henshaw, T. F.; Cheek, J.; Broderick, J. B. *J. Am. Chem. Soc.* **2000**, *122*, 8331−8332.
(30) Cosper, N. J.; Booker, S. J.; Ruzicka, F.; Frey, P. A.; Scott, R. A. *Biochemistry* **2000**, *39*, 15668−15673.
(31) Abragam, A.; Bleaney, B. *Electron Paramagnetic Resonance of Transition Ions*; Dover Publications: New York, 1986.
(32) Lee, H.-I.; Dexter, A. F.; Fann, Y.-C.; Lakner, F. J.; Hager, L. P.; Hoffman, B. M. *J. Am. Chem. Soc.* **1997**, *119*, 4059−4069.
(33) Tierney, D. L.; Martasek, P.; Doan, P. E.; Masters, B. S. S.; Hoffman, B. M. *J. Am. Chem. Soc.* **1998**, *120*, 2983−2984.

studies of AdoMet binding to the enzyme in the equilibrium geometry associated with the catalytically active paramagnetic $[4Fe-4S]^{1+}$ state of the cluster, denoted [1+/AdoMet]. We have also studied the interactions between AdoMet and the *diamagnetic* $[4Fe-4S]^{2+}$ state via ENDOR. To do this, the $[4Fe-4S]^{2+}$ PFL-AE sample is first frozen in the presence of AdoMet and then γ-irradiated at 77 K to produce the $[4Fe-4S]^{1+}$ valency cluster cryogenically trapped in the geometry of the 2+ state, denoted $[2+/AdoMet]_{red}$.[34−40] The results described here provide the first direct spectroscopic evidence for a close association between AdoMet and the $[4Fe-4S]^{1+}$ and $[4Fe-4S]^{2+}$ cluster states of PFL-AE. The implications of these results for the mechanism of [4Fe−4S] cluster mediated reductive cleavage of AdoMet are discussed.

Materials and Methods

Materials. AdoMet synthetase overproducing strain DM22(pK8) was a generous gift from Dr. George D. Markham (Fox Chase Cancer Center). Methyl-D_3-L-methionine and methyl-^{13}C-L-methionine were purchased from Isotec Inc. ATP and inorganic pyrophosphatase were purchased from Sigma. These and all other chemicals were of the highest purity obtainable from commercial sources.

PFL-AE was purified from overexpressing *E. coli* BL21(DE3)pLysS/pCal-n-AE3 as previously described,[18] except that 1 mM DTT was included in all buffers. Protein, iron, and sulfide assays were done as perviously described.[18,41,42]

For the preparation of AdoMet synthetase, a single colony of DM22-(pK8) was used to inoculate 50 mL of LB media containing 30 μg/mL oxytetracycline (LB/Tet). This culture was grown for 12−14 h to saturation and then used to inoculate 700 mL of LB/Tet in each of five 2800 mL Fernbach culture flasks. The cultures were grown at 37 °C with vigorous shaking for 12−14 h before harvesting by centrifugation at 11000*g*. The cell paste was stored frozen at −80 °C. AdoMet syntheses were carried out using crude extracts of DM22(pK8) cells. To prepare the crude extract for the synthesis reactions, cell paste was suspended (∼3 mL/g cells) in 100 mM Tris−HCl, pH 8.0 containing 1 mM EDTA. Lysozyme was added to 50 μg/mL, and the suspension was incubated at room temperature for 30 min. (Phenylmethyl)sulfonyl fluoride (PMSF) was added to a final concentration of 0.1 mM. Cells were lysed by sonication in an ice bath. The suspension was centrifuged at 27000*g* for 20 min, and the clarified extract was stored at −80 °C until needed.

Synthesis of Isotopically Labeled AdoMet. AdoMet syntheses were carried out using modifications of a procedure described previously.[43] Reactions (10 mL) were carried out at room temperature with moderate stirring in 100 mM Tris−HCl, pH 8.0 containing 50 mM KCl, 26 mM $MgCl_2$, 13 mM ATP, 1 mM EDTA, 8% β-mercaptoethanol, 10 mM isotopically labeled methionine, a small amount of inorganic pyrophosphatase (∼0.25 U), and 1 mL of AdoMet synthetase lysate (approximately 13 mg total protein). All reagents were added in the order listed. The reaction was monitored by thin-layer chromatography on silica plates developed in butanol/acetic acid/water (4:1:1). The reaction was terminated, typically after 12−16 h, by addition of 1 mL of 1 M HCl, and precipitated protein was removed by centrifugation at 27000*g* for 20 min at 4 °C. The supernatant was decanted and split in half. Half of the supernatant was loaded onto a SOURCE 15S cation exchange column (Pharmacia), which had been charged with 1 M HCl and equilibrated with water. The column was run with a linear gradient of 0−1 M HCl, and AdoMet eluted from 0.4 to 0.6 M HCl as a distinct peak. The other half of the supernatant was then run through the same procedure. Fractions containing products were pooled, lyophilized, and stored at −80 °C until needed.

Methyl-D_3-AdoMet (CD_3-AdoMet) was synthesized by the above procedure using 98% enriched L-methionine-methyl-D_3. The yield was 38.5 mg (87.9%) for 10 mL of 10 mM reaction. ^{1}H NMR (D_2O): δ 2.18−2.39 (m, Hβ & Hβ'), 3.32−3.42 (m, Hγ & Hγ'), 3.52−3.62 (m, Hα), 3.76−3.98 (m, H5′, H5" & H4′), 4.38−4.73 (m, H3′ & H2′), 6.01 (d, J = 3.91 Hz, H1′), 8.32 (s, H2 & H8) ppm. The ^{2}H labeling was confirmed by the absence of a methyl peak in the ^{1}H NMR, as well as the presence of a methyl peak at 3.03 ppm in the ^{2}H NMR.

Methyl-^{13}C-AdoMet ($^{13}CH_3$-AdoMet) was synthesized by the above procedure using 99% enriched L-methionine-methyl-^{13}C. The yield was 37.5 mg (86.0%) for a 10 mL reaction of 10 mM substrate. ^{1}H NMR (D_2O): δ 2.20−2.35 (m, Hβ & Hβ'), 2.62 & 3.11 (d, J = 146.49, (−)-$^{13}CH_3$), 3.37−3.43 (m, Hγ & Hγ'), 3.44−3.58 (m, Hα), 3.77−4.01 (m, H5′, H5″ & H4′), 4.38−4.71 (m, H3′ & H2′), 6.01 (d, J = 3.91, H1′), 8.32 (s, H2 & H8) ppm. The ^{13}C labeling was confirmed by the distinct large splitting of the methyl peak in the ^{1}H NMR, as well as the presence of a large ^{13}C peak at 23.78 ppm in the ^{13}C NMR. Integration of the NMR signal showed an approximately 95:5 ratio of the natural (−)-AdoMet to the (+)-AdoMet isomer.

NMR Spectroscopy. ^{1}H, ^{13}C, and ^{2}H NMR spectra were recorded at room temperature on a Varian Inova-300 or a VXR-300 spectrometer.

Preparation of E·AdoMet Samples for EPR and ENDOR. All procedures were carried out anaerobically in an inert atmosphere glovebox (Mbraun) with O_2 levels ≤3 ppm. Purified PFL-AE was exchanged into 50 mM Tris−HCl, 200 mM NaCl, 1 mM DTT, pH 8.5, and glycerol was added to a final concentration of 20−25% (v/v). To prepare the reduced $[4Fe-4S]^+$ PFL-AE, 1 molar equiv of sodium dithionite was added to the PFL-AE, and then 5-deazariboflavin was added in the dark to 200 μM final concentration. The sample was illuminated for 1 h in an EPR tube on ice using a 500 W halogen lamp. After illumination, the protein sample was quickly mixed with 2 equiv of AdoMet or labeled AdoMet on ice, transferred to the EPR and ENDOR tubes, and flash-frozen in liquid nitrogen in the glovebox. The samples so prepared are designated as [1+/AdoMet] to indicate that AdoMet is added to the $[4Fe-4S]^+$ form of PFL-AE.

To make the AdoMet complex with the $[4Fe-4S]^{2+}$ state of PFL-AE, purified PFL-AE containing $[4Fe-4S]^{2+}$ as the major cluster form was exchanged into 50 mM Tris−HCl, 200 mM NaCl, 1 mM DTT, pH 8.5 buffer. In the inert atmosphere glovebox, glycerol was added to 20% (v/v), and the PFL-AE was mixed with 2 equiv of either CD_3-AdoMet or $^{13}CH_3$-AdoMet. The samples, designated [2+/CD_3-AdoMet] and [2+/$^{13}CH_3$-AdoMet], were loaded into ENDOR tubes and flash-frozen in liquid nitrogen in the glovebox. The samples were then γ-irradiated at 77 K to produce the 1+ valency cluster trapped in the geometry of the 2+ state, as discussed elsewhere,[34−40] and these samples are hereafter referred to as $[2+/CD_3\text{-AdoMet}]_{red}$ and $[2+/^{13}CH_3\text{-AdoMet}]_{red}$.

EPR and ENDOR Spectroscopy. Pulsed ENDOR spectra (35 GHz) were recorded on a spectrometer described earlier,[44] equipped with a helium immersion dewar, and all the measurements were carried out at approximately 2 K. Pulsed ENDOR measurements employed the three-pulse Mims ENDOR sequence ($\pi/2-\tau-\pi/2-T-\pi/2-\tau-$echo), where the RF was applied during the interval T.

(34) Symons, M. C. R.; Petersen, R. L. *Proc. R. Soc. London B* **1978**, *201*, 285−300.
(35) Davydov, R. M. *Biofizika* **1980**, *25*, 203−207.
(36) Kappl, R.; Höhn-Berlage, M.; Hüttermann, J.; Bartlett, N.; Symons, M. C. R. *Biochim. Biophys. Acta* **1985**, *827*, 327−343.
(37) Leibl, W.; Nitschke, W.; Hüttermann, J. *Biochim. Biophys. Acta* **1986**, *870*, 20−30.
(38) Davydov, R.; Kappl, R.; Hutterman, R.; Peterson, J. *FEBS Lett.* **1991**, *295*, 113−115.
(39) Davydov, R.; Kuprin, S.; Graslund, A.; Ehrenberg, A. *J. Am. Chem. Soc.* **1994**, *116*, 11120−11128.
(40) Davydov, R.; Valentine, A. M.; Komar-Panicucci, S.; Hoffman, B. M.; Lippard, S. J. *Biochemistry* **1999**, *38*, 4188−4197.
(41) Beinert, H. *Methods Enzymol.* **1978**, *54*, 435−445.
(42) Beinert, H. *Anal. Biochem.* **1983**, *131*, 373−378.
(43) Park, J.; Tai, J.; Roessner, C. A.; Scott, A. I. *Bioorg. Medicinal Chem.* **1996**, *4*, 2179−2185.
(44) Davoust, C. E.; Doan, P. E.; Hoffman, B. M. *J. Magne. Reson.* **1996**, *119*, 38−44.

For a nucleus (N) of spin $I = {}^1/_2$ (^{13}C, ^{1}H) interacting with a $S = {}^1/_2$ paramagnetic center, the first-order ENDOR spectrum for a single molecular orientation is a doublet,

$$\nu_{\pm} = \nu_N \pm A/2 \quad (2)$$

centered at ν_N, the Larmor frequency, and split by A, the orientation dependent hyperfine constant, when $\nu_N > A/2$, as is true here for ^{1}H and ^{13}C nuclei. Similarly, for a deuteron ($I = 1$) where $\nu_D > A/2$, as is true here, the first-order ENDOR resonance condition can be written

$$\nu_{\pm}(\pm) = \nu_D \pm \frac{A}{2} \pm \frac{3P}{2} \quad (3)$$

where P is the orientation-dependent quadrupolar splitting. This is the case with ^{2}H nuclei in the present study. The full hyperfine tensor of a coupled nucleus, both principal values and orientation parameters (Euler angles) with respect to the g-tensor frame, is obtained by simulating the 2-D pattern of orientation-dependent ENDOR spectra recorded across the EPR envelope using the procedures and program described elsewhere.[45−49] The computer simulation and analysis of the frozen-solution ENDOR spectra used in the present work are described in the same references.

For a nucleus with hyperfine coupling, A, the Mims techniques have a response R that depends on the product, $A\tau$, according to the equation

$$R \sim [1 - \cos(2\pi A\tau] \quad (1)$$

This function has zeroes, corresponding to minima in the ENDOR response (hyperfine suppression holes), at $A\tau = n$; $n = 0, 1, 2, ...$, and maxima at $A\tau = (2n + 1)/2$; $n = 0, 1, 2, ...$,[45,46] The hyperfine couplings suppressed by the holes at $A = n/\tau$, $n = 1, 2, 3, ...$ can be adjusted by varying τ. However, the central, $n = 0$, hole at $\nu = \nu_N$ persists regardless. This can be of significance in distinguishing a tensor that is dominated by anisotropic interactions from one that is dominated by isotropic ones. The latter would never predict ENDOR intensity near ν_N, while the former does so for certain orientations. By suppressing intensity near ν_N, the $n = 0$ Mims hole diminishes the differences between the two cases.

Experimental Results

EPR Spectroscopy. PFL-AE purified anaerobically in the presence of DTT, as is done here, contains primarily $[4Fe-4S]^{2+}$ clusters, with small quantities (<1% of total iron based on EPR spin quantitation) of $[3Fe-4S]^+$ clusters. Reduction of PFL-AE using photoreduced 5-deazariboflavin as described in Materials and Methods typically yields $[4Fe-4S]^+$ enzyme in 300−400 μM concentrations based on EPR spin quantitation. The presence of AdoMet produces dramatic effects on the EPR signal of the $[4Fe-4S]^{1+}$ cluster, as shown in Figure 1. In the absence of AdoMet, the $[4Fe-4S]^+$ cluster of PFL-AE gives a rhombic EPR signal (g = 2.02, 1.94, 1.88). However, if AdoMet is added to the reduced $[4Fe-4S]^+$-PFL-AE, the observed EPR signal is nearly axial (g = 2.01, 1.88, 1.87). Radiolytic cryoreduction at 77 K of PFL-AE treated with AdoMet in the 2+ state produced the 1+ cluster trapped in the structure characteristic of the precursor 2+ state. The state denoted $[2+/AdoMet]_{red}$ has an EPR signal identical to that of the [1+/AdoMet] state (not shown), suggesting that [2+/AdoMet] and [1+/AdoMet] have the same structures.

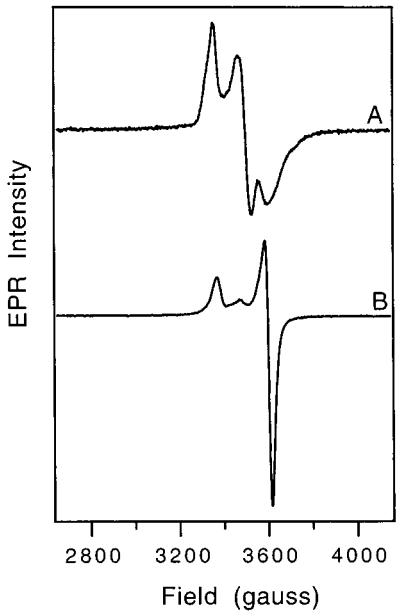

Figure 1. 9.5 GHz CW EPR spectra of PFL-AE photoreduced with deazariboflavin as described in the text. (A) PFL-AE (0.7 mM) photoreduced for 1 h. The signal accounts for 197 μM $[4Fe-4S]^+$ based on EPR spin quantitation, and has been multiplied by 3 for comparison purposes. (B) PFL-AE (0.78 mM) photoreduced for 1 h, followed by addition of two molar equivalents of AdoMet. The signal accounts for 416 μM $[4Fe-4S]^+$ based on EPR spin quantitation. Conditions: T = 12 K, power = 20 μW, gain = 2×10^4, frequency = 9.483 (A) or 9.476 (B), modulation amplitude = 8.231 (A) or 9.571 (B).

^{2}H and ^{13}C ENDOR. The observed effect of AdoMet on the EPR signal of the catalytically relevant $[4Fe-4S]^+$ cluster could reflect either a close association between AdoMet and the cluster or more remote allosteric perturbations of the cluster. These possibilities were investigated using ENDOR spectroscopy.

The ^{2}H ENDOR spectra of [1+/CD_3-AdoMet] and $[2+/CD_3\text{-AdoMet}]_{red}$, Figure 2, and the corresponding ^{13}C spectrum of [1+/$^{13}CH_3$-AdoMet] and $[2+/^{13}CH_3\text{-AdoMet}]_{red}$, Figure 3, immediately demonstrate that the cofactor sits close to the cluster in both the 1+ and 2+ states. The ^{2}H spectra of [1+/CD_3-AdoMet] taken at $\mathbf{g}_\perp$ and $\mathbf{g}_\parallel$, Figure 2, both show a well-defined deuteron pattern that overlays a less-intense signal seen in the unlabeled [1+/AdoMet] sample (see Supporting Information); this latter is assigned to "$\Delta m = 2$" transitions from weakly coupled ^{14}N, as seen in similar Fe−S clusters.[50] In the ^{2}H spectrum collected at $g_\perp$, the breadth of the signal is 1.1 MHz, which, when corrected for unresolved ^{2}H quadrupole splitting of ~0.1 MHz (based on the known value for quadrupole coupling for CD_3),[51] corresponds to a substantial ^{1}H coupling of ~6−7 MHz. For comparison, this coupling is approximately half that of water bound to a low-spin heme.[52] Such an interaction could not arise from an AdoMet bound at a remote site and influencing the cluster EPR spectrum by an allosteric

(45) Mims, W. B. In *Electron Spin−Echoes*; Geschwind, S., Ed.; Plenum Press: New York, 1972.
(46) Mims, W. B. *Proc. R. Soc. London* **1965**, *283*, 452−457.
(47) Hoffman, B. M.; Martinsen, J.; Venters, R. A. *J. Magn. Reson.* **1984**, *59*, 110−123.
(48) Hoffman, B. M.; Venters, R. A.; Martinsen, J. *J. Magn. Reson.* **1985**, *62*, 537−542.
(49) Hoffman, B. M. *Acc. Chem. Res.* **1991**, *24*, 164−170.
(50) Houseman, A. L. P.; Oh, B. H.; Kennedy, M. C.; Fan, C.; Werst, M. M.; Beinert, H.; Markley, J. L.; Hoffman, B. M. *Biochemistry* **1992**, *31*, 2073−2080.
(51) Ragle, J. L.; Mokarram, M.; Presz, D.; Minott, G. *J. Magn. Reson.* **1975**, *20*, 195−213.
(52) Fann, Y.-C.; Gerber, N. C.; Osmulski, P. A.; Hager, L. P.; Sligar, S. G.; Hoffman, B. M. *J. Am. Chem. Soc.* **1994**, *116*, 5989−5990.

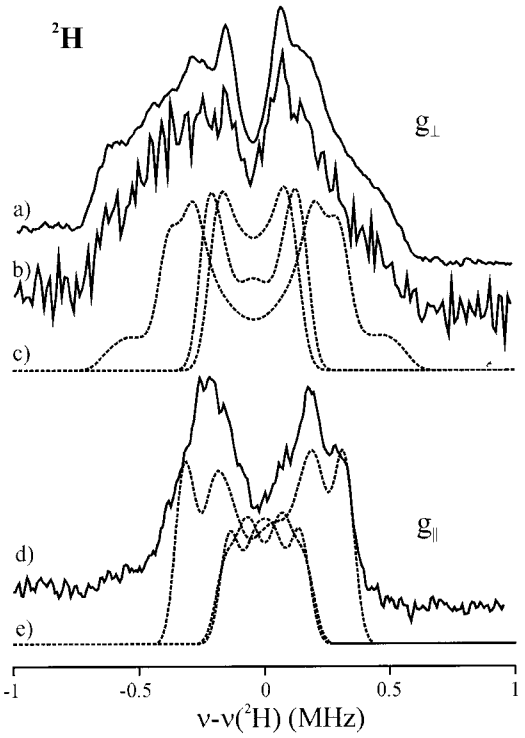

Figure 2. 35 GHz Mims pulsed-ENDOR spectra of PFL-AE with methyl-D_3-AdoMet; (a) and (d) photoreduced sample; (b) cryoreduced sample. The spectra at $\mathbf{g}_\perp$ have been scaled to the height of the natural abundance ^{57}Fe peaks visible to higher frequency of the ^{13}C signals. Conditions: $T = 2$ K, $\nu_{MW} = 34.8$ GHz, MW pulse lengths = 80 nS, $\tau = 456$ ns, RF pulse length = 60 μs, repetition rate = 30 Hz. Each spectrum consists of 256 points with each point an average of 240−300 transients. (c) and (e) Simulations (dashed lines) with dipolar **A** tensors. Closest ^{2}H: $T = 0.6$ MHz (corresponding to $R = 3.1$ Å for $K = 1.0$), $\alpha = \beta = 30°$, $\gamma = 0°$; $P = 0.1$ MHz, $\alpha = \beta = \gamma = 0°$. More distant methyl deuterons: $r(Fe_k-D) = 4.7$ Å, representative value of $K = 1.6$, angles tetrahedrally disposed, orientations: $\alpha = 19°$, $\beta = 20°$, $\gamma = 0$ and $\alpha = 30°$, $\beta = 54°$, $\gamma = 0$, quadrupole as above. Mims suppression effects included.

process; at a minimum it requires the AdoMet lie adjacent to the cluster. That AdoMet binds with the same geometry to both the 1+ and 2+ clusters is confirmed by the ^{2}H ENDOR spectra of $[2+/AdoMet]_{red}$, which is trapped in the geometry of [2+/AdoMet]. As illustrated in Figure 2, the ^{2}H spectra of [1+/CD_3-AdoMet] and $[2+/CD_3\text{-AdoMet}]_{red}$ are indistinguishable.

^{13}C ENDOR spectra collected from [1+/$^{13}CH_3$-AdoMet] and $[2+/^{13}CH_3\text{-AdoMet}]_{red}$, Figure 3, lead to identical conclusions. The two labeled samples exhibit identical hyperfine-split doublets centered at the ^{13}C Larmor frequency and arising from coupling to ^{13}C of the labeled AdoMet lying adjacent to the cluster. The spectra also show ENDOR signals from natural abundance ^{57}Fe. These are assigned to the ν_+ transition of a single iron with a coupling of $\mathbf{A}(^{57}Fe) = 26$ MHz, which is similar to that of the labile Fe site in aconitase ES ($\mathbf{A}(^{57}Fe) = 29$ MHz). The existence of this signal is useful because it provides a method for normalizing spectra from natural-abundance and ^{13}C-enriched samples, by scaling to the ^{57}Fe signal.

Field Dependence of ^{13}C ENDOR. Details of the AdoMet binding have been obtained by analysis of the 2D patterns of 35 GHz Mims pulsed ^{13}C ENDOR spectra from [1+/$^{13}CH_3$-AdoMet] and ^{2}H spectra from [1+/CD_3-AdoMet], each collected across the entire EPR envelope. Figure 3 presents the 2D set of Mims pulsed ^{13}C ENDOR spectra; at each field the

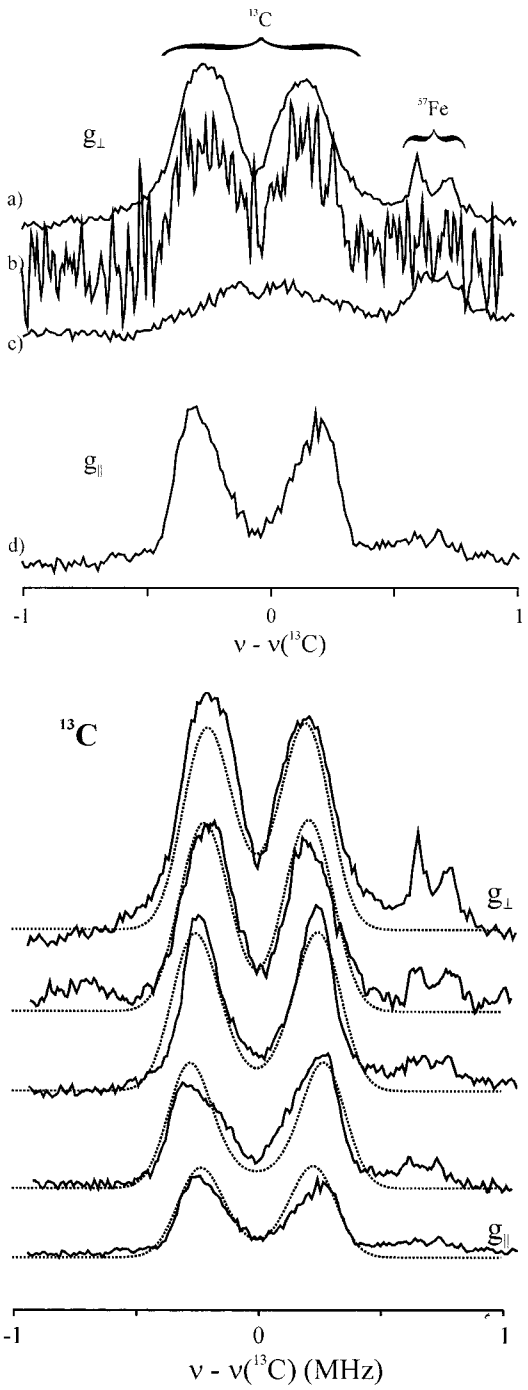

Figure 3. Upper panel: 35 GHz Mims pulsed-ENDOR spectra of PFL-AE (a) with methyl-^{13}C-AdoMet, photoreduced, at $\mathbf{g}_\perp$, (b) with methyl-^{13}C-AdoMet, (d) with methyl-^{13}C-AdoMet, photoreduced, at $\mathbf{g}_\parallel$. Irradiated at 77 K, at $\mathbf{g}_\perp$ (c) with natural abundance ^{13}C-AdoMet at $\mathbf{g}_\parallel$. Experimental conditions as for Figure 2 except that $\tau = 600$ nS and number of transients = 600. Lower panel: field dependence data with conditions as above (full line) and simulation (dashed line). Simulation parameters: $\mathbf{A} = [-0.6, 0.4, -0.5]$, $\alpha = \beta = 30°$, $\gamma = 0°$; EPR line width = 170 MHz, ENDOR line width = 0.2 MHz; $\tau = 600$ ns, Mims suppression effects included.

spectrum is normalized to the 2-pulse electron-spin−echo (ESE) signal intensity. We note that with the value, $\tau = 600$ ns, employed in the Mims ENDOR pulse sequence, the $n = 1$ "Mims suppression holes" fall sufficiently far from the ^{13}C Larmor frequency (holes at $\Delta\nu(^{13}C) = \nu\pm - \nu_C = \pm 0.833$ MHz) that they do not significantly distort the observed ^{13}C pattern. However the $n = 0$ "hole", centered *at* the ^{13}C Larmor

frequency ($\Delta\nu(^{13}C) = 0$ MHz) regardless of τ, has a major impact on the observed signals and, as a result, it is essential to incorporate Mims suppression into the simulations. This procedure has not been thoroughly studied, and we find that the "simple" appearance of the Mims suppression holes can be altered by spin-diffusion effects. However, by simple incorporation of the Mims formula in the simulation program and by use of carefully normalized spectra, it is possible to analyze the experiments persuasively. In particular, by requiring the simulations to reproduce the relative peak intensities from field to field in the 2D pattern, as well as the frequencies, it is possible to characterize the dipolar part of the hyperfine interaction reasonably well; the attention to intensities is particularly important at fields and for orientations where the hyperfine coupling approaches zero and may change sign. As shown in Figure 3, through systematic efforts we obtained excellent simulations of the peak positions *and* intensities with a ^{13}C hyperfine tensor that has principal values, $\mathbf{A}(^{13}C) = [-0.6(1), +0.4(1.5), -0.5(1)]$ MHz[53] and Euler angles relative to the **g**-tensor frame of $\theta = 30°$, $\psi = 30°$. We note that although A_1 and A_3 do not appear to differ within error, the errors are correlated. To reproduce the curvature of the outer edges of the 2D plot, A_1 must be ~0.1 MHz larger than A_3, and thus $\mathbf{A}(^{13}C)$ is constrained to be nonaxial.

The ^{13}C tensor can be decomposed into the sum of an isotropic part, $\mathbf{a}_{iso}(^{13}C) = -0.23$ MHz, and two, mutually perpendicular, dipolar tensors, $\mathbf{T}(^{13}C) = [-0.33, +0.66, -0.33] \equiv [-T_C, 2T_C, -T_C]$ MHz, and $\mathbf{t}(^{13}C) = [-0.03, -0.03, +0.06] \equiv (-)[-t, -t, 2t]$ MHz. The former we assign to the through-space dipolar interaction between the ^{13}C and spin of the cluster; the latter we assign to the "local" interaction with the spin on the ^{13}C itself whose presence is disclosed by the isotropic term. The hyperfine tensor, thus, can be decomposed into the "nonlocal" dipolar interaction with the cluster and a "local" term that arises from spin density on the ^{13}C, $\mathbf{A}(^{13}C)_{loc} = -[|\mathbf{a}_{iso}(^{13}C)|\mathbf{1} + \mathbf{t}(^{13}C)]$. The presence of spin density at the methyl group of AdoMet, as manifest in this local term, *requires* that AdoMet lie in contact with the cluster, weakly interacting with it through an incipient bond/antibond. The opposite signs of the through-space and local contributions suggests that the spin on the methyl carbon is not directly delocalized from the cluster but involves spin polarization through an intervening atom, presumably the sulfonium sulfur of AdoMet.

The nonlocal through-space coupling tensor, **T**, contains information about the geometry of AdoMet binding. The dipole interaction between the cluster and nucleus j of AdoMet, here the ^{13}C of the labeled methyl, can be written as

$$H_{HF} = \hat{S}\cdot\sum_j \mathbf{T}_j\cdot\hat{I}_j$$

where

$$\mathrm{T}_j = g_e\beta_e g_N^j\beta_N\sum_{i=1}^{4}\frac{K_i}{r_{ij}^3}\mathbf{t}_{ij} \approx \frac{g_e\beta_e g_N^j\beta_N}{r_{kj}^3}K_k\mathbf{t}_{kj} \equiv T_j\mathbf{t}_{kj} \qquad (4)$$

Here K_i is the spin-projection coefficient for Fe_i of the spin-coupled $S = {}^1/_2$ cluster, the Fe_i-Nuc_j distance is r_{ij}, and $\mathbf{t}_{kj}$ is the dimensionless through-space electron−nuclear dipolar matrix. Calculations indicate that only the dipole coupling to the nearest iron ion, k, need be considered to a first approximation, as indicated in eq 4, and hence the dipole coupling to nucleus j is characterized by the parameter, $T_j \equiv g\beta g_N^j\beta_N K_k/r_{jk}^3$.

Table 1. Alternate Results for Fe−Methyl Distances from Eq 4 for $T(^2H) = 0.60$ MHz and $T(^{13}C) = 0.33$ MHz

$\lvert K\rvert$[a]	$r(^2H\text{–}Fe_n)$[b] (Å)	$r(^{13}C\text{–}Fe_n)$ (Å)
1.78	3.8(1)	5.0(6)
1.60	3.7(1)	4.9(6)
1.57	3.6(1)	4.9(6)
0.86	3.0(1)	4.0(6)

[a] Vector coupling coefficients for Fe adjacent to the methyl group, these being four possible values as described in the text. The uncertainties are those in T obtained in the simulation. [b] Nearest methyl proton (deuteron) with distances calculated within the "dipole" model (see text).

The determination of r_{C-k} from the parameter T_C for the ^{13}C -methyl requires knowledge of K_k. Mössbauer spectroscopic studies of [1+(AdoMet)] in progress do not yet provide the K_i for the four Fe ions, and therefore we consider the known spin coefficients of the 1+ cluster of substrate-bound aconitase (ES), which also has a labile, noncysteine cluster ligand; these are $|K| = 0.86$, 1.57, 1.60, and 1.78.[54] When interpreting the ^{13}C dipolar interaction constant, $T_C = 0.33$ MHz, in this way, the point-dipole-calculated distance between the methyl ^{13}C and Fe_k of the cluster then would take one of four rather well-defined distances, depending on which value of K is associated with Fe_k; these are listed in Table 1. The range of possible values for r_{C-k} given the uncertainties in the simulations and including the full range for the values of K then spans the range ~4−5 Å (Table 1).

Field Dependence of ^{2}H ENDOR. The ^2H and ^{13}C ENDOR data have been tested for self-consistency by analysis of the 2D set of ^2H Mims pulsed ENDOR spectra collected for [1+/CD_3-AdoMet]. Figure 2 includes the spectra at both $\mathbf{g}_\perp$ and $\mathbf{g}_\parallel$; the intervening spectra (not included) show that the breadth of the pattern decreases monotonically from $\mathbf{g}_\perp$ to $\mathbf{g}_\parallel$. The deuteron spectrum is not highly resolved but the hyperfine splitting at $\mathbf{g}_\perp$ is roughly twice that of the splitting at $\mathbf{g}_\parallel$. For a CD_3 moiety, the maximum ^2H quadrupole coupling is only $P \sim 0.1$ MHz[51] and for a ^2H spectrum as broad as that shown in Figure 2, the shape is dominated by the hyperfine interaction to the three deuterons ($j = 1-3$). The spectra are compatible with a surprisingly simple model in which the AdoMet is bound alongside the cluster and the outer features of the CD_3 ENDOR response are governed by the through-space dipolar interaction between the closest methyl deuteron and the spin density on a single Fe ion of the cluster; the inner part of the pattern is filled in by intensity from the other two methyl-group deuterons.

The outer features of the field-dependent ^2H pattern can be modeled by the interaction of one deuteron with a single iron Fe_k where the C−D1 bond points at Fe_k[55] with the dipole-coupling parameter, $T_D \equiv g\beta g\beta_\nu K_n/r_{D-k}^3 = 0.60$ MHz. The calculated point-dipole distance between the closest methyl deuteron and the Fe_k of the cluster again take one of four rather narrowly defined distances that span the range ~3.0−3.8 Å. Contributions from the more remote deuterons were calculated

(53) The relative signs are fixed by experiment. The absolute sign is not and is chosen to make the dipolar interaction positive.

(54) Telser, J.; Huang, H.; Lee, H.-I.; Adams, M. W. W.; Hoffman, B. M. *J. Am. Chem. Soc.* **1998**, *120*, 861−870.

(55) Same Euler angles for D1 and C.

under the constraint of this location for D1 and tetrahedral geometry around the methyl carbon, along with simple assumptions as to the orientation of the AdoMet; it also depends somewhat on the choice of K_k. As shown by the calculated spectra in Figure 2, the data can be represented by summing the contributions from the three methyl deuterons calculated in this fashion. The parameters used for the calculations are given in the legend to Figure 2.

While the analysis for the ^{13}C is robust, the analysis for the deuterons is not unique, however. This is because the behavior of the D1 pattern cannot be well-modeled at small couplings due to unavoidable uncertainties about the contributions from the D2, D3 signals, and the effects of the $n = 0$ "Mims hole". Thus, the spectra can be fit with an alternate model for D1 in which an isotropic coupling makes a significant contribution to the ^2H observed pattern. While such simulations themselves are not unique, a representative simulation that describes the outer spectral features utilized a tensor, $\mathbf{A} = [0.3, 0.3, 1.0]$ MHz, corresponding to an isotropic coupling $a = 0.53$ MHz and an anisotropic contribution of the form $[-0.23, -0.23, 0.47]$ MHz. In this model, the lack of resolution in the small coupling region of the ^2H spectra again is attributed to the presence of signals from the other two deuterons which, although chemically equivalent, would have different isotropic couplings. The isotropic coupling to deuteron j likely varies as $\cos^2 \theta_j$, where θ_j is the dihedral angle between the π orbital on S that acquires spin from the cluster and the C−D_j bond.[56] For example, if D1 has the maximum possible coupling ($\theta = 0$), the other two will have 4-fold smaller values ($\theta = \pm 2\pi/3$, $\cos^2 \theta = {}^1/_4$), thus contributing intensity near the center of the spectrum as required by experiment.

In principle, one might hope to distinguish between the two models by examining the modulation depth of the ^2H ESEEM time-domain trace at X-band frequencies. However, attempts to do this were not successful. While the quality of the simulations based on the two models is similar, there are some grounds for preferring one of them. As shown in Table 1, the values of T_C and of T_D derived from the dipolar interpretation of the ^2H data yield a model where the C−D1 bond (bond length of ~ 1 Å) points toward Fe_k. The "isotropic" model of the ^2H 2D pattern yields a correspondingly diminished T_D that corresponds to a value of $r(^2H-Fe_k)$ that, however, is comparable to that of $r(C-Fe_k)$. Thus, we favor the purely dipole model as the better approximation.[57] However, the $r(D1-Fe_k)$ predicted from the value of T_D derived from the model with substantial isotropic ^2H coupling are close to those for $r(^{13}C-Fe_k)$; for example, for the covalent model, choosing the K values in descending order produces distances of 4.5, 4.4, 4.3, and 3.5 Å, all of which are within the range of the distances deduced for $r(^{13}C-Fe_k)$.

Discussion

PFL-AE has been shown to utilize the $[4Fe-4S]^+$ state of the cluster to catalyze the reductive cleavage of AdoMet and subsequent generation of the glycyl radical of PFL. During this catalytic turnover, the $[4Fe-4S]^+$ cluster is oxidized to $[4Fe-4S]^{2+}$, thereby indicating that the cluster is the source of the electron necessary for reductive cleavage of AdoMet.[29] Taken at face value, these results might suggest that the iron−sulfur cluster in PFL-AE is serving a simple electron-transfer role, much like the iron−sulfur clusters found in numerous electron-transfer proteins. Indeed, such a role has been proposed for the iron−sulfur cluster in the related anaerobic ribonucleotide reductase activating enzyme.[58] However, it is also possible that the redox chemistry is occurring not by remote electron transfer, but through covalent chemistry between the cluster and AdoMet. As a first step toward probing the details of the mechanism of radical generation by PFL-AE, we have investigated the interaction between AdoMet and the iron−sulfur cluster of PFL-AE. Significantly, it is possible to probe the interaction of AdoMet with the catalytically active $[4Fe-4S]^+$ of PFL-AE, because PFL-AE/$[4Fe-4S]^+$ does not reductively cleave AdoMet in the absence of PFL.[29,59]

Scheme 2. Model for the Interaction of AdoMet with the [4Fe−4S] of PFL-AE

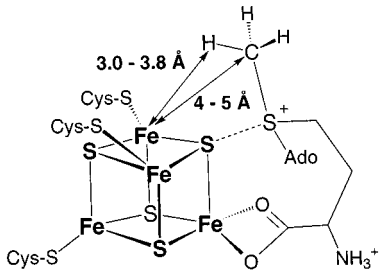

Initial evidence that AdoMet might be closely associated with the cluster was provided by EPR spectroscopy (Figure 1): the presence of AdoMet produces a clear effect on the EPR signal of the $[4Fe-4S]^+$ state of PFL-AE, causing the distinctly rhombic signal to become nearly axial. Such a dramatic change in the EPR signal of the cluster would be consistent with AdoMet coordinating to an iron of the cluster or otherwise closely associating with the cluster. A change in signal such as that observed in Figure 1, however, also could be explained if AdoMet binds at a remote site and causes changes in the cluster through allosteric interactions. The EPR spectrum of the $[2+/AdoMet]_{red}$ is identical to that of [1+/AdoMet], indicating that the AdoMet binds in the same fashion to both 1+ and 2+ states.

To determine the nature of AdoMet binding to the 2+ and 1+ states of PFL-AE, we have carried out ^2H and ^{13}C ENDOR studies of specifically labeled AdoMets bound to the enzyme. Since the catalytic turnover of AdoMet involves chemistry occurring at the sulfonium center, we reasoned that atoms in the vicinity of the sulfonium are most likely to be located close to the cluster, and thus AdoMet labeled at the sulfonium methyl was used in this study. The observation of substantial ^2H and ^{13}C hyperfine couplings from labeled AdoMet bound to the 1+ cluster of PFL-AE clearly demonstrates that AdoMet binds adjacent to the 4Fe cluster (Figures 2 and 3). Moreover, the observation of identical spectra from the 1+ and cryoreduced 2+ enzyme further shows that the position of AdoMet relative to the Fe−S cluster in PFL-AE is identical in the oxidized and reduced states. Modeling of the dipolar interactions between the cluster and the methyl-^{13}C and -^2H of AdoMet shows that

(56) Werst, M. M.; Davoust, C. E.; Hoffman, B. M. *J. Am. Chem. Soc.* **1991**, *113*, 1533−1538.
(57) We do not rule out a small isotropic contribution.
(58) Padovani, D.; Thomas, F.; Trautwein, A. X.; Mulliez, E.; Fontecave, M. *Biochemistry* **2001**, *40*, 6713−6719.
(59) Knappe, J.; Neugebauer, F., A.; Blaschkowski, H. P.; Gänzler, M. *Proc. Natl. Acad. Sci U.S.A.* **1984**, *81*, 1332−1335.

Scheme 3. Proposed Mechanism for the Reductive Cleavage of AdoMet and Generation of the PFL Glycyl Radical by PFL-AE

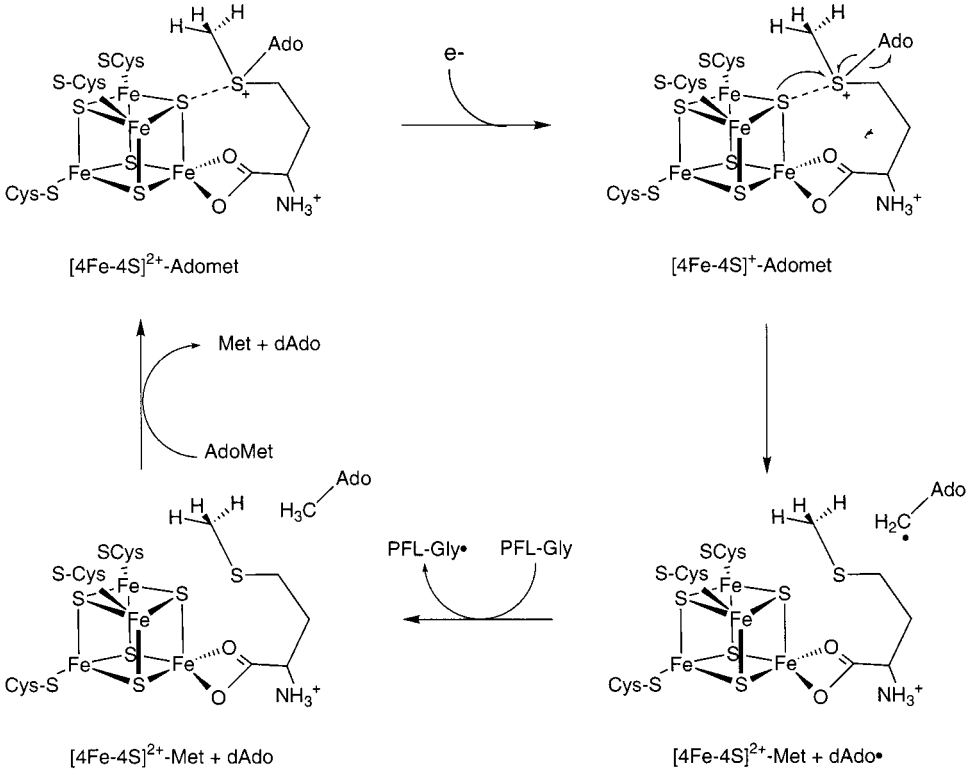

the methyl group of AdoMet is quite close to one of the irons of the cluster, as close as ~3.0 Å for the methyl proton and no more than ~4−5 Å for the methyl carbon, with the calculated value dependent on the identity of the nearby Fe. Most intriguingly, the existence of an isotropic contribution to the ^{13}C tensor requires that there be overlap between orbitals on the cluster and on AdoMet, namely, that there are incipient covalent interactions between AdoMet and the cluster. The most plausible interpretation is that this interaction is of a dative character, between a negatively charged sulfide of the cluster and the positively charged sulfur of AdoMet, as shown in Scheme 2.

An alternative model for the interaction of AdoMet with the cluster would involve a direct coordination of the sulfonium of AdoMet to an iron of the cluster. This would be analogous to the recent proposal by Cosper et al. for lysine aminomutase, in which the sulfonium of AdoMet is poised near (but not coordinated to) the unique iron site of the cluster, and where the Met formed by reductive cleavage coordinates to the unique site.[30] We disfavor this model for PFL-AE primarily for electrostatic reasons. Noodleman and Case have shown by using DFT methods that most of the increased electron density associated with going from a 2+ to a 1+ cluster resides on the sulfide and cysteinal sulfurs, with very little being associated with the irons of the cluster.[60] The significantly larger electron density and partial negative charge at the sulfurs of the cluster, corresponding to partial positive charge at the irons, suggests that the positively charged sulfonium would prefer to interact with a sulfide. The electron density changes at sulfur proposed by Noodleman and Case also point to the likelihood of sulfur-based, rather than iron-based, redox chemistry in iron−sulfur clusters.[60] The ENDOR results presented here do not preclude the possibility of an Fe−sulfonium interaction in PFL-AE such as proposed in LAM. However, it should be noted that in LAM, AdoMet functions as a reversibly cleaved cofactor, while in PFL-AE, AdoMet acts as a substrate that undergoes irreversible C−S bond cleavage. Any apparent differences in the mode of interaction of AdoMet with the cluster in PFL-AE and LAM may simply reflect the differences in the roles of AdoMet.

If, as we are proposing here, the sulfonium of AdoMet interacts with a sulfur, not an iron, of the cluster, then what is the role for the unique (noncysteine-coordinated) iron site that appears to be conserved among these enzymes? Partly on the basis of electrostatics and partly on the precedent with aconitase,[24−27] we propose that the methionine carboxylate of AdoMet coordinates to this iron, displacing whatever ligand is present in the absence of AdoMet; this proposal is currently under further investigation in our laboratories through ENDOR studies using AdoMet selectively labeled at the carboxylate position with ^{17}O.[61]

On the basis of the cluster−AdoMet interaction shown in Scheme 2, we propose a mechanism for the Fe−S/AdoMet-driven radical chemistry catalyzed by PFL-AE (Scheme 3). As demonstrated by our ENDOR results, AdoMet binds to the $[4Fe-4S]^{2+}$ state of PFL-AE, close enough to the cluster to provide overlap between orbitals on AdoMet and on the cluster. Reduction of the cluster produces the AdoMet-bound $[4Fe-4S]^{+}$-PFL-AE without a change in structure. These results are in contrast with the proposal that AdoMet does not bind near to the 2+ or 1+ cluster of lysine aminomutase in the absence of substrate but that substrate binding "recruits" AdoMet to the vicinity of the cluster.[30] According to Scheme 3, in the

(60) Noodleman, L.; Case, D. A. *Adv. Inorg. Chem.* **1992**, *38*, 423−470.

(61) ENDOR is also being used to probe the possibility of other coordinating groups, such as the methionine amino or the adenosyl hydroxyl groups of AdoMet, using appropriately labeled ^{15}N or ^{17}O AdoMets.

presence of AdoMet the [1+/AdoMet] complex then undergoes inner-sphere electron transfer from the cluster to AdoMet, via the sulfide-sulfonium interaction, which results in homolytic cleavage of the sulfonium-adenosyl bond. This leaves methionine coordinated to the cluster, and an adenosyl radical that can abstract the hydrogen atom from Gly-734 of PFL.

Summary

The result of these investigations is a structural model of AdoMet bound to both 1+ and 2+ states of PFL-AE in which a cluster sulfide and the AdoMet sulfur are adjacent, with weak dative orbital overlap, while the AdoMet methyl-group carbon lies ∼4−5 Å from an Fe ion. This model is illustrated by the structure presented in Scheme 2 and leads to the proposed catalytic mechanism of Scheme 3.

Acknowledgment. We thank Dr. R. Davydov for sample irradiation, C. E. Davoust for expert technical assistance, Prof. J. Telser for useful discussions, and the NIH ((GM54608 (J.B.B.), HL13531 (B.M.H.)) for support.

Supporting Information Available: Figure showing the field dependence of ^{2}H Mims ENDOR spectra from PFL-AE with methyl-D_3-AdoMet and with unlabeled AdoMet (PDF). This material is available free of charge via the Internet at http://pubs.acs.org.

JA012034S